J Mater Sci (2007) 42:9239–9244
DOI 10.1007/s10853-007-1902-5

Visible-light responsive zinc ferrite doped titania photocatalyst for methyl orange degradation

Ping Cheng · Changsheng Deng · Mingyuan Gu · Wenfeng Shangguan

Received: 11 July 2006 / Accepted: 31 May 2007 / Published online: 27 July 2007

Abstract Visible-light responsive zinc ferrite doped titania (ZFDT) photocatalysts were prepared by sol-gel method. Diffuse Reflectance Spectroscopy (DRS) result shows that the absorption edge of ZFDT has moved to the visible spectrum range and a very large redshift occurs in comparison with the undoped titania. X-ray diffraction (XRD) results show that zinc ferrite can prevent the transformation of titania from anatase to rutile when the content of zinc ferrite is above 1.5%; while the phase transformation is promoted when its content is below 1.5%. In the latter case, zinc ferrite was assumed to exist as separate zinc and ferric cations in the lattice of titania in the form of oxides, both of which promote the phase transformation as previously reported in other literatures. Field emission scanning electron micrography (FE-SEM) shows that the average particle size of 1.5%$ZnFe_2O_4/TiO_2$ calcined at 500 °C is about 70 nm. The photocatalytic experimental results exhibit that ZFDT powders can effectively photodegrade methyl orange under visible light irradiation and the maxium photoactivity is achieved when the amount of zinc ferrite is 1.5%.

P. Cheng (✉) · C. Deng
State Key Lab of New Ceramics and Fine Processing, Institute of Nuclure & New Energy Technology, Tsinghua University, Beijing 100084, China
e-mail: chengpingtsinghua@yahoo.com.cn

M. Gu · W. Shangguan
State Key Laboratory of MMCs, Shanghai Jiaotong University, Shanghai 200030, China

Introduction

In recent years, titania has been widely studied for its applications in photocatalysis, solar cells and hydrogen production [1–6]. Generally, photocatalytic degradation of organic compounds includes the following processes. An electron is excited from the valence band to the conduction band (CB) of TiO_2 by absorption of light with energy equal to or greater than the band gap of the TiO_2 semiconductor. The separated photoinduced electrons and holes transfer to the semiconductor surface efficiently. At the surface, electrons react with acceptors (usually O_2 dissolved in the solution) to produce oxidant species, for example hydroxyl radicals. Meanwhile, holes react with donors (H_2O, OH^-) to produce oxidant species. Oxidant species produced from electrons and holes have strong oxidizing abilities and can directly oxidize organic compounds into CO_2 and H_2O. However, titania is a wide band gap semiconductor (3.03 eV for rutile and 3.18 eV for anatase) and can only absorb about 5% of sunlight in the ultraviolet region, which greatly limits its practical applications. Extensive efforts have been made in the development of titanium oxide photocatalysts that can efficiently utilize sunlight or indoor light (the so-called second-generation photocatalyst) [7–12].

Recently, it has been found that spinel zinc ferrite is another semiconductor (band gap 1.9 eV) that has potential applications in the conversion of sunlight. However, because of the lower valence band potential and poor property in photoelectric conversion, zinc ferrite cannot be used directly in the photocatalytic destruction of toxic organic compounds [13]. Titania has high photoactivity and superior property in photoelectric conversion, while zinc ferrite is sensitive to visible light. So the compound of these two semiconductors, which utilizes the special properties of nanoparticles and the coupling between them,

may become a new type of composite having high utility of sunlight, high photoactivity and high efficiency of photoelectric conversion.

In this paper, zinc ferrite doped titania (ZFDT) powders were prepared by sol-gel method with the aim of extending the light absorption spectrum toward the visible region. The photocatalytic degradation of methyl orange, chosen as an aromatic model molecule, has been performed under both ultraviolet and visible light irradiation. The microstructure has been characterized using X-ray diffraction (XRD) and Field emission scanning electron micrography (FE-SEM) methods.

Experimental

Preparation of ZFDT powders

Five different kinds of ZFDT nanopowders (with the weight percentage of zinc ferrite ranging from 0.06% to 6%) were prepared by sol-gel process. Tetrabutyl titanate, zinc nitrate and ferric nitrate were used as precursors of titania and zinc ferrite, respectively. Firstly, zinc nitrate, ferric nitrate and citric acid in a 1:2:2.5 molar ratio were dissolved together in ethanol to produce a clear solution. The concentration of zinc ion in the solution was 0.15 M. The mixture was vigorously stirred for 2 h and then was diluted to achieve the required percentage of zinc ferrite.

During the synthesis of titania sol, hydrochloric acid was used as the catalyst. The molar ratio of $Ti:H_2O:HCl:C_2H_5OH$ equals to 1:2.5:1:15. In order to avoid strong hydrolysis reactions, $Ti(OBu^n)_4$ was diluted with half of the prescribed amount of ethanol at first, then water and catalyst dissolved in the remaining ethanol were added dropwise to the ethanolic solution of alkoxide with continuous stirring. Simultaneously, the prescribed diluted zinc ferrite solution was added dropwise to the titania sol. Different zinc ferrite/titania sols were obtained by varying the weight percentage of zinc ferrite after vigorous stirring for several hours. The gels were calcined at the temperature range 350–750 °C for 2 h, and then ground into fine powders. For comparison, pure titania and pure zinc ferrite powders were also prepared by the above described method.

Measurements and analysis methods

The Diffuse Reflectance Spectroscopy (DRS) spectra of the powders were recorded with a TU-1901 dual beam UV–VIS spectrometer, equipped with an integrating sphere attachment for their diffuse reflectance in the range of 230–850 nm. $BaSO_4$ was used as the standard in all measurements. XRD patterns were recorded with a Rigaku D/max3A diffractometer with Cu K_α radiation over the 2θ range of 10–90° to identify the phase structure of samples. The crystal size was estimated using Scherrer equation. Field emission scanning electron micrography was performed in a LEO 1551VP system.

Set-up of photocatalytic reaction

The photocatalytic activities of the samples were evaluated by the decomposition of methyl orange under both ultraviolet and visible light irradiation. A 250 W high pressure Hg lamp was used as the light source. The Hg lamp produces light peaked at around 365 nm covering both ultraviolet and visible light region. A 1 M $NaNO_2$ solution was utilized to screen the ultraviolet radiation when conducting visible light experiments (After filtered out by 1 M $NaNO_2$ solution, the wavelength of light is longer than 400 nm). The initial concentration of methyl orange in a quartz reaction vessel was fixed at 25 mg/L and the catalyst loading was 5 g/L. The extent of methyl orange decomposition was determined by measuring the absorbance at approximately 465 nm using a 756MC UV-VIS spectrometer. Prior to illumination, the suspension was magnetically stirred in the dark for 30 min to establish the adsorption-desorption equilibrium at room temperature. During irradiation, stirring was maintained to keep the mixture in suspension. At regular intervals, samples were taken from the suspension. And the liquid was analyzed after the solid photocatalyst particles were removed by centrifuge.

Results and discussion

Figure 1 presents DRS spectra of TiO_2, $ZnFe_2O_4/TiO_2$ and $ZnFe_2O_4$ calcined at 500 °C. It can be seen that the reflectance curves for $ZnFe_2O_4/TiO_2$ composite powders

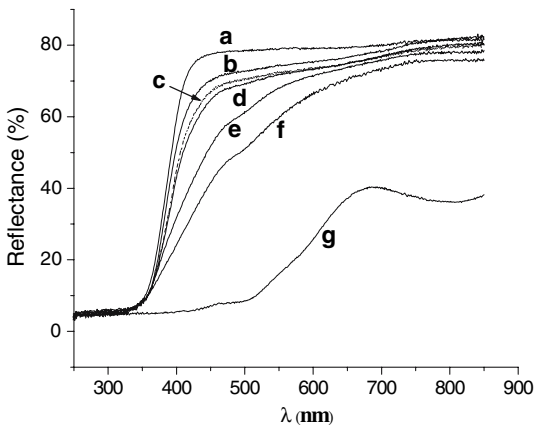

Fig. 1 DRS spectra for ZFDT calcined at 500 °C (the weight percentage of zinc ferrite: a: 0; b: 0.06%; c: 0.15%; d: 0.3%; e: 1.5%; f: 3%; g: 100%.)

are between those for pure titania and pure zinc ferrite. Furthermore, with the increase of the amount of zinc ferrite, the reflectance in the visible range of 400–700 nm decreases dramatically. This result proves that, upon addition of zinc ferrite particles to titania, the absorption of the composite powders in the visible spectrum range increases significantly in comparison with that of the undoped titania. This means that the composite powders are sensitive to visible light. The obvious large redshift of the $ZnFe_2O_4/TiO_2$ powders is considered to be due to two factors. One of these comes from the mixing effect of band gaps of the composite semiconductor. When anatase titania with a relatively broad band gap mixed with zinc ferrite, a narrow band gap material, the band gap of $ZnFe_2O_4/TiO_2$ composite semiconductor will be located between the band gaps of these two semiconductors, i.e., it shifts to a lower energy, as compared with that of titania. Since the added amount of zinc ferrite is very low, ranging from 0.06 wt.% to 3 wt.% (wt.% is an abbreviation of weight percentage), the mixing effect alone cannot account for the whole large redshift. The other factor is considered to be the interface effect. Due to the interfacial coupling effect between zinc ferrite and titania grains, zinc ferrite can induce lattice defects on the surface of TiO_6 octahedra, which will serve as the centres of bound excitons [14].

Figure 2 illustrates the XRD patterns of $0.15\%ZnFe_2O_4/TiO_2$, $0.3\%ZnFe_2O_4/TiO_2$, $1.5\%ZnFe_2O_4/TiO_2$, $6\%ZnFe_2O_4/TiO_2$ and pure $ZnFe_2O_4$ powders calcined at 500 °C. There are sharp and strong peaks of anatase phase at $2\theta = 25.3°$ in XRD patterns of all $ZnFe_2O_4/TiO_2$ samples. Meanwhile, a small peak of rutile phase appears in the XRD patterns of $0.15\%ZnFe_2O_4/TiO_2$ and $0.3\%ZnFe_2O_4/TiO_2$ at $2\theta = 27.4°$. It is inferred that zinc ferrite can effectively promote the transformation from anatase to rutile when its content is less than 1.5%. Meanwhile, zinc ferrite peaks can be detected in the XRD patterns of $1.5\%ZnFe_2O_4/TiO_2$ and $6\%ZnFe_2O_4/TiO_2$ although they are very weak.

Figure 3 illustrates the XRD patterns of $1.5\%ZnFe_2O_4/TiO_2$ calcined at 350–750 °C (a–e) and pure TiO_2 (f) heated at 550 °C. The rutile peak is already present in pure titania powder when it is heated at 550 °C. However there are no rutile peaks in $1.5\%ZnFe_2O_4/TiO_2$ powders until it is calcined at 650 °C. The anatase to rutile phase transformation takes place at an annealing temperature T_a above 650 °C and completes at 750 °C. This means that zinc ferrite retards the transformation onset temperature of titania from anatase to rutile by 100 °C in comparison with the undoped titania. It has been reported that sol-gel derived titania undergoes anatase-to-rutile phase transformation at temperatures ranging from 550 °C to 800 °C and the temperature range of transformation spans 250 °C [15]. So the transformation onset temperature is 100 °C higher and the temperature range of transformation is 150 °C narrower than that reported in the literature. This means that zinc ferrite prevents the transformation of titania from anatase to rutile and narrows the temperature range of the transformation when its content is above 1.5 wt.%. To understand the role of zinc ferrite in the transformation, an analysis of the crystalline structure of anatase and rutile is necessary. The comparison of the two crystal structures of titania indicates that the transformation involves a collapse of the open anatase structure to a closed rutile structure, with a volume change of about 8%. This process takes place by the rupture of two of the six Ti–O bonds of the titanium coordination octahedral in anatase to form new bonds in rutile, as indicated earlier by Shannon [16]. For

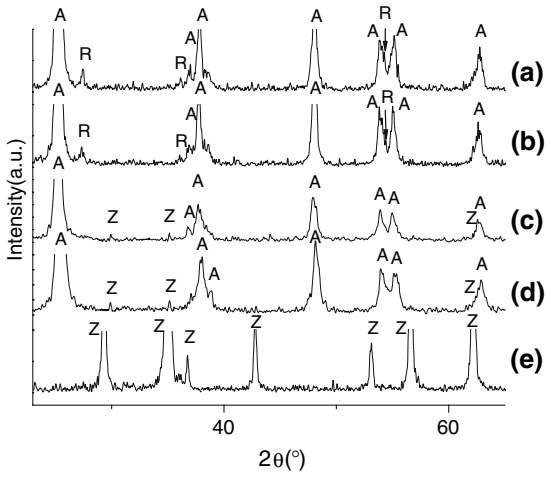

Fig. 2 XRD patterns of ZFDT powders calcined at 500 °C (A-anatase, R-rutile, Z-zinc ferrite, the amount of zinc ferrite: a: 0.15%; b: 0.3%; c: 1.5%; d: 6%; e: 100%.)

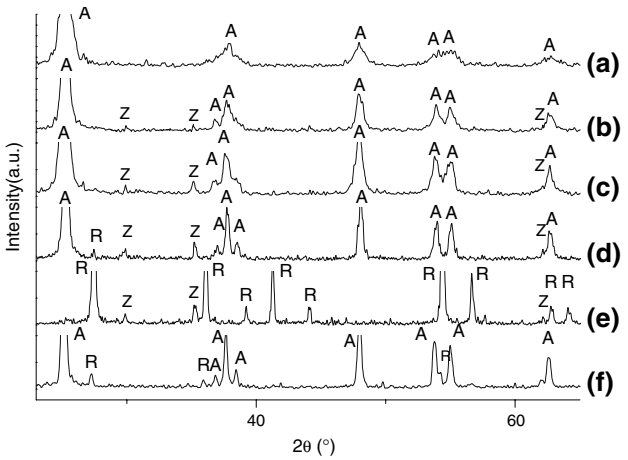

Fig. 3 XRD patterns of $1.5\%ZnFe_2O_4/TiO_2$ calcined at various temperatures (A-anatase, R-rutile, Z-zinc ferrite: a: 350°C; b: 500°C; c: 600°C; d: 650°C; e: 750 °C and f: pure TiO_2 calcined at 550 °C

ZFDT, the interface formed between the spinel zinc ferrite and anatase titania holds back the formation of the new bonds in rutile and the phase transformation from anatase to rutile in ZFDT powder is retarded.

However, the result in Fig. 3 shows that the transformation of titania from anatase to rutile is promoted when the content of zinc ferrite is less than 1.5 wt.%. In general, phase transformation of nucleation and growth type proceeds through three different stages. The first stage is nucleation or, strictly speaking, embryo formation. The second stage is the growth of this embryo to reach the critical nuclei size. The final stage is the stable growth of crystals. In this stage, critical nuclei can grow to large crystallites of the transformed phase by consuming the parent phase. It is reported that the additive ferric oxide can promote the anatase-to-rutile transformation to be finished in a fairly narrow temperature range [17]. Yuan et al. [18] have reported that the addition of zinc oxide can lower the onset temperature of phase transformation from anatase to rutile. In the present study, it is inferred that zinc ferrite cannot nucleate or grow due to the breakage of the abundant network of titania when its content is below 1.5 wt.%. The enhancement of phase transformation of titania is caused by zinc and ferric cations solid-soluted in the titania lattice, as reported in [17–18]. When the content of zinc ferrite is above 1.5 wt.%, spinel zinc ferrite grains are formed after heat treatment, which is verified by the XRD results, and prevent the transformation of titania from anatase to rutile due to interfacial effect.

The crystallite size of powders was determined from the broadening of corresponding X-ray diffraction peaks by using Scherrer's formula $D = (K\lambda)/(\beta\cos\theta)$, where λ is the wavelength of the X-ray radiation ($\lambda = 0.15418$ nm), K the Scherrer constant (K = 0.9), θ X-ray diffraction peak and β the full-width at half-maximum (FWHM) of the (101) plane of anatase titania (in radians), which is corrected for the instrumental broadening ($\beta_0 = 0.00122$ rad) prior to calculation of its particle size broadening [19]. When calcined at 350, 500, 600 and 650°C, the calculated anatase grain sizes of 1.5%$ZnFe_2O_4/TiO_2$ were 6, 12, 15, and 20 nm, respectively.

The morphology of 1.5%$ZnFe_2O_4/TiO_2$ powder calcined at 500 °C was observed by FE-SEM. Figure 4 shows that the calcined powder consisted of loose particles with an average size of 70 nm. The size of these particles was different from the XRD calculated size of 12 nm. The difference resulted from that nanoparticles tended to aggregate into "domains" in local regions.

Figures 5 and 6 shows the effect of the amount of doped zinc ferrite on the specific photocatalytic performance of the ZFDT photocatalysts for the oxidative degradation of methyl orange dissolved in distilled water under visible light irradiation ($\lambda > 400$ nm) and ultraviolet plus visible light, respectively. Photo-degradation of methyl orange in the presence of ZFDT powders in the dark, under visible light and under ultraviolet plus visible light irradiation, respectively, was also evaluated. It was found that no degradation for the methyl orange in the presence of ZFDT in the dark occurred. Also no degradation was observed for methyl orange when the solution was placed under radiation without the addition of ZFDT powders.

Under visible light irradiation, the photocatalytic degradation of MO proceeded on the $ZnFe_2O_4/TiO_2$ photocatalysts (Fig. 5b–f). After 4 h photodegradation reaction excited by visible light, 84% methyl orange were destroyed on the 1.5%$ZnFe_2O_4/TiO_2$ samples, while only 10%

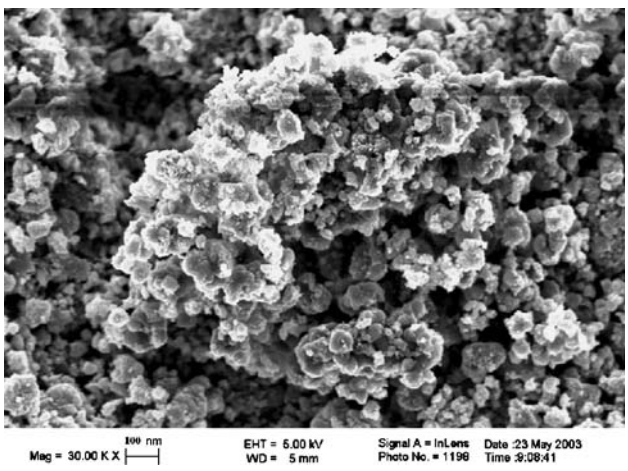

Fig. 4 FE-SEM image of 1.5%$ZnFe_2O_4/TiO_2$ calcined at 500 °C

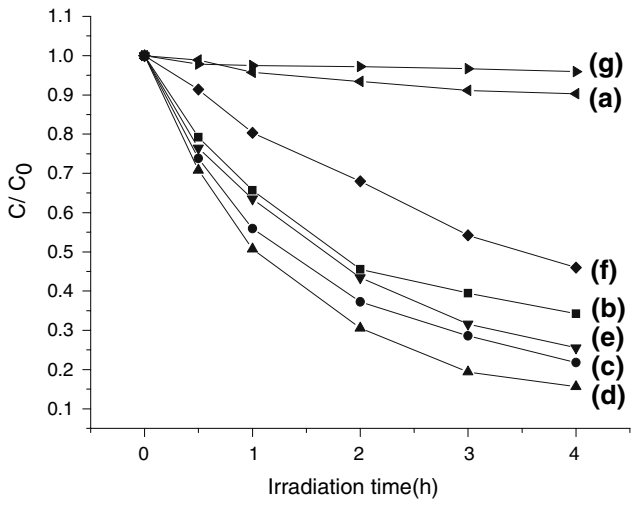

Fig. 5 The effect of the amount of zinc ferrite on the photocatalytic reactivities of the $ZnFe_2O_4/TiO_2$ photocatalysts for the degradation of methyl orange under visible light irradiation ($\lambda > 400$ nm) (the amount of zinc ferrite in wt.%: a: 0; b: 0.15; c: 0.3; d: 1.5; e: 3; f: 6; g: 100.)

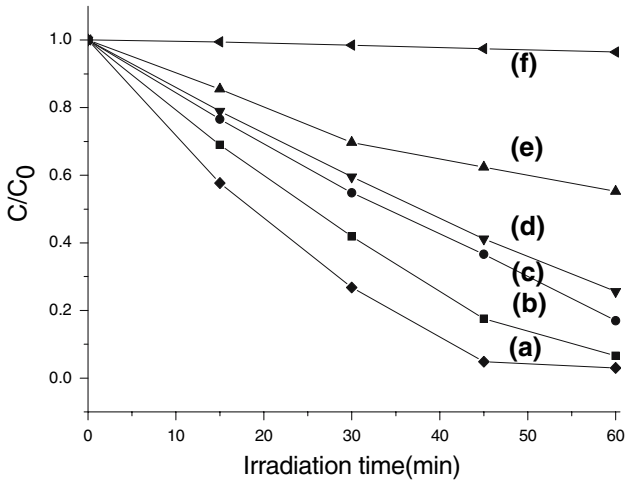

Fig. 6 The effect of the amount of zinc ferrite on the photocatalytic reactivities of the $ZnFe_2O_4/TiO_2$ photocatalysts for the degradation of methyl orange under ultraviolet plus visible light irradiation (the amount of zinc ferrite wt.%: a: 0; b: 0.06; c: 0.15; d: 0.3; e: 6; f: 100.)

methyl orange were degraded on the undoped pure TiO_2 (Fig. 5a). The degradation of methyl orange on undoped TiO_2 under visible light irradiation is attributed to the photobleaching process [20]. Anatase titania cannot be directly excited by visible light due to its 3.2 eV band-gap, but the photobleaching reaction still occurred under TiO_2/dye/visible-light system due to dye molecule acting as photosensitizer. The electron from the excited dye molecule was injected into the CB of the TiO_2, and the cation radical formed at the dye surface quickly undergoes degradation reaction. The photocatalytic reactivity under visible light irradiation increases constantly with the increase of the amount of the doped zinc ferrite. The maximum photocatalytic reactivity is observed when the amount of zinc ferrite is 1.5 wt.%. However, the excess amount of zinc ferrite leads to the decrease of the photocatalytic reactivity. As shown in Fig. 1, the absorption bands of the $ZnFe_2O_4/TiO_2$ shift to the longer wavelength region with the increase of the amount of zinc ferrite. This efficient shift of absorption band can increase the number of photons that can be absorbed by the catalyst and utilized for the photocatalytic reaction. Furthermore, as shown by the XRD result in Fig. 2, there was rutile in $0.15\%ZnFe_2O_4/TiO_2$ and $0.3\%ZnFe_2O_4/TiO_2$, but no peaks of rutile were found in the XRD patterns of $1.5\%ZnFe_2O_4/TiO_2$. So the phase composition also accounts for the higher photoactivity of $1.5\%ZnFe_2O_4/TiO_2$ since anatase is generally thought to have higher photoactivity than rutile. However, the excess amount of zinc ferrite can cover the surface of the catalyst and suppress the photocatalytic reaction. These results indicate that the moderate amount of zinc ferrite is suitable for efficient photocatalytic reaction under visible light irradiation. However, under ultraviolet plus visible light irradiation (Fig. 6), the photocatalytic degradation of methyl orange on the ZFDT photocatalysts was poorer than the undoped TiO_2 and the loss of photoactivity of the catalyst increases with the increase of the amount of doped zinc ferrite. Compared to undoped TiO_2, the decrease of photoactivity of the ZFDT photocatalysts under ultraviolet plus visible light irradiation can be attributed to the low photoactivity of ZFDT under ultraviolet light. Although the high-pressure Hg lamp used in the paper produces light covering both ultraviolet and visible light region, ultraviolet light peaked at around 365 nm accounts for a large proportion. Therefore, photodegradation of MO under ultraviolet plus visible light irradiations is mainly caused by excitation from ultraviolet light while photodegradation by excitation from visible light can be negligible. However, compared with undoped TiO_2, the absorption of ZFDT for the visible light plays a predominant role in the increase of photoactivity of ZFDT as discussed in Fig. 5. So the decrease of photoactivity of the ZFDT under ultraviolet plus visible light is understandable. The improvement of irradiation condition including choosing solar simulator as light source, as well as the detailed mechanism study are in progress.

Conclusion

ZFDT nanopowders with various amount of zinc ferrite were prepared by sol-gel method. DRS results show that the absorption edge of ZFDT has moved to the visible spectrum range, and a very large redshift occurs with increasing the amount of zinc ferrite in comparison with the undoped titania. The photocatalytic degradation of methyl orange indicates that ZFDT powders can effectively photodegrade methyl orange under visible light irradiation and the maximum photoactivity is achieved when the amount of doped zinc ferrite is 1.5 wt.%. However, the photoactivity of ZFDT powders was lower than the undoped original TiO_2 photocatalyst and the loss of photoactivity increases with the increase in the amount of doped zinc ferrite under ultraviolet plus visible light irradiation. The effect of zinc ferrite doping on the anatase-to-rutile phase transformation of TiO_2 was also reported. XRD results show that zinc ferrite can inhibit the transformation of titania from anatase to rutile when the weight percentage of zinc ferrite is above 1.5%; while the phase transformation is promoted when it is below 1.5%. FE-SEM image shows that average particle size of $1.5\%ZnFe_2O_4/TiO_2$ calcined at 500 °C was about 70 nm. The calculated crystalline size according to Scherrer's formula is 12 nm. The difference in size was mainly due to aggregation effect of nanoparticles.

References

1. Zeltner WA, Fu X, Anderson MA (1995) Appl Catal B 6(3):209
2. Jung KY, Park SB (2000) Appl Catal B 25(4):249
3. Jean-Marie H, Chantal G, Jean D, Corinne L, Sixto M, Julian B (2002) Appl Catal B 35(4):281
4. Goeringer S, Chenthamarakshan CR, Rajeshwar K (2001) Electrochem Commun 3:290
5. Thaminimulla CTK, Takata T, Hara M, Kondo JN, Domen K (2000) J Catal 196:362
6. Bessekhouad Y, Mohammedil M, Trari M (2002) Solar Energy Mater Solar Cells 73:339
7. Asahi R, Morikawa T, Ohwaki T (2001) Science 293:269
8. Khan SUM, Al-Shahry M, Ingler WB Jr (2002) Science 297:2243
9. Anpo, M, Takeuchi M (2003) J Catal 216:505
10. Anpo M, Takeuchi, M, Ikeue K, Doshi S (2002) Curr Opin Solid St Mater Sci 6(5):381
11. Ihara T, Miyoshi M, Iriyama Y, Matsumoto O, Sugihara S (2003) Appl Catal B 42:403
12. Xie Y, Yuan C (2003) Appl Catal B 46:251
13. Valenzuela MA, Bosch P, Jiménez-Becerrill J, Quiroz O, Páez AI (2002) J Photochem Photobiol A 148:177
14. Saraf LV, Patil SL, Ogale SB (1998) J Mod Phys 12:2635
15. Ding X-Z, Liu X (1997) Mat Sci Eng A-Struct 224:210
16. Shannon RD (1964) J Appl Phys 35:3414
17. Ding XZ (1995) Ph. D, Thesis, Insititute of Solid Physics, Chinese Academy of Science, p 53
18. Yuan Z, Zhang L (1998) Nanostruct Mater 10:1127
19. Rainho JP, Rocha J, Carlos LD (2001) J Mater Res 16:2369
20. de GJ, Soler-Illia AA, Candel RJ, Regazzoni AE, Blesa MA (1997) Chem Mater 9:184